# Probing Pauli blocking with shot noise in resonant tunneling diodes: Experiment and theory

I. A. Maione,[1] M. Macucci,[1] G. Iannaccone,[1] G. Basso,[1] B. Pellegrini,[1] M. Lazzarino,[2] L. Sorba,[2,3] and F. Beltram[3]
[1]*Dipartimento di Ingegneria dell'Informazione, Università di Pisa, via Caruso 16, I-56122 Pisa, Italy*
[2]*Laboratorio TASC INFM-CNR, S. S. 14 km 163, 5, I-34012 Basovizza, Italy*
[3]*Scuola Normale Superiore, Piazza dei Cavalieri 7, I-56100 Pisa, Italy*
(Received 3 January 2007; published 28 March 2007)

The Pauli exclusion principle is one of the fundamental tenets of quantum mechanics and determines the structure of matter at the atomic and molecular levels. Here, we show that Pauli blocking, a consequence of the exclusion principle according to which electron transitions are inhibited if the arrival state is occupied by another electron, has an observable effect on shot noise in resonant tunneling diodes. We measure a double valley feature in the plot of the noise suppression factor (the "Fano" factor) as a function of the applied voltage, which has been theoretically predicted a few years ago but has never been observed, and which suggests that Pauli blocking must be considered in the evaluation of transport in mesoscopic and nanoelectronic devices.

DOI: 10.1103/PhysRevB.75.125327 PACS number(s): 73.50.Td, 73.21.−b, 73.40.Gk

## I. INTRODUCTION

Shot noise is a fundamental physical effect resulting from the granularity of charge carriers: if carriers are emitted into and cross the device randomly, without any correlation, full shot noise is observed, with a current power spectral density $S_I=2qI$, where $q$ is the electron charge and $I$ is the average current. This result, as stated in Schottky's theorem,[1] is the consequence of the variance of a Poisson process being equal to its average value. The presence of correlations between carriers produces deviations from such a behavior: noise can be suppressed if the motion of carriers is made more regular by negative correlations[2] or increased if fluctuations are enhanced by particle bunching.[2] The ratio of the measured shot-noise power spectral density to that predicted by Schottky's theorem is usually defined as Fano factor.

The double barrier resonant tunneling diode (RTD) is an ideal testbed for the investigation of such phenomena, since it exhibits, depending on the bias region, both phenomena: shot noise suppression and enhancement.[3–6]

Here, we focus on the case of Fano factor less than unitary, which is observed for an applied voltage lower than that corresponding to the voltage peak. Shot-noise suppression is, in general, the consequence of correlations either due to Coulomb interaction or due to Pauli blocking.[7]

A few years ago, some of us predicted a specific signature of the interplay between Coulomb interaction and Pauli blocking, to be observed in the Fano factor of a resonant tunneling diode at low bias and low temperature (below 14 K).[8] While experimental results were still missing, additional theoretical papers appeared on the subject.[9,10]

In this paper, we are able to present experimental data exhibiting such an effect, an intuitive physical interpretation, and detailed numerical simulations confirming our interpretation.

Pauli blocking has no effect on the dc and ac properties of electronic devices, therefore its actual role has often been debated in the literature.[11,12] The possibility offered by shot noise of observing Pauli blocking in action confirms its role as a very sensitive probe of electron-electron-interaction.[13]

## II. MODEL

Let us first provide a simple physical picture of the phenomenon. A typical conduction-band profile of a resonant tunneling diode under bias is shown in Fig. 1. As can be seen, four transition mechanisms are present: two from the contacts to the well through barrier $i$ ($i=1,2$), described by the number of electron transitions per unit time (generation rate) $g_i$, and two from the well to the contacts through barrier $i$, described by the recombination rate $r_i$. The net dc current $I$ is

$$I=q(g_2-r_2)=q(r_1-g_1), \tag{1}$$

for current continuity through the device. When the applied bias is much larger than the thermal voltage, electrons enter the well only through barrier $2(g_1=0)$.

The rate $g_2$ is obtained by summing up over all possible transition rates $\nu_{\alpha\beta}$ from any state $\alpha$ in the emitter to any state $\beta$ in the well, weighted by the probability that the initial state $\alpha$ is occupied ($f_\alpha$) and that the final state $\beta$ is unoccupied $(1-f_\beta)$, and $r_2$ can be obtained with an analogous procedure,

$$g_2=\sum_{\alpha,\beta}\nu_{\alpha\beta}f_\alpha(1-f_\beta), \quad r_2=\sum_{\alpha,\beta}\nu_{\alpha\beta}f_\beta(1-f_\alpha). \tag{2}$$

Pauli blocking is of course responsible for the $(1-f)$ factors in Eq. (2) but, as it is well known, does not play any role in the DC behavior. Indeed, substituting Eq. (2) into Eq. (1), we have

$$I=q(g_2-r_2)=q\sum_{\alpha,\beta}\nu_{\alpha\beta}(f_\alpha-f_\beta), \tag{3}$$

which is the same result as we would obtain if the $1-f$ factors were removed from Eq. (2). The issue of whether the $(1-f)$ factors (the so-called "Pauli blocking" factors) have to be included has been debated in the literature.[11,12]

Shot noise, on the other hand, is sensitive to electron-electron interaction and therefore to Pauli blocking.

In Ref. 14 a useful formula for the power spectral density of the shot-noise current $S$ has been derived [Eq. (35)], which we rewrite below as

$$\frac{S}{2q^2}=\left(\frac{\tau_1}{\tau_1+\tau_2}\right)^2(r_1+g_1)+\left(\frac{\tau_2}{\tau_1+\tau_2}\right)^2(g_2+r_2), \tag{4}$$

 

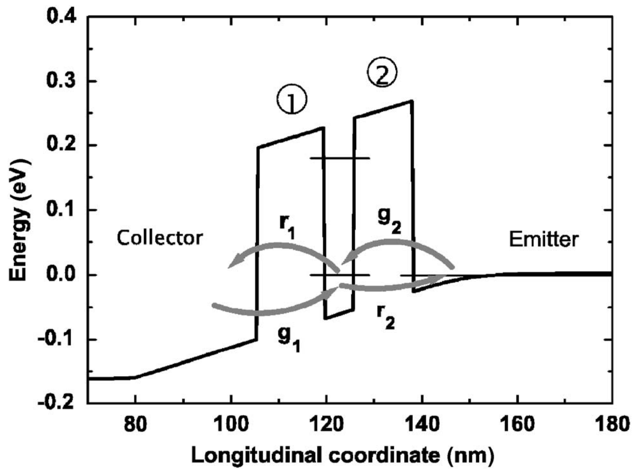


FIG. 1. Theoretical conduction-band profile of the resonant tunneling diode under investigation at the temperature of 6 K and a voltage bias of 0.17 V.

where

$$\tau_1 \equiv \left[\frac{\partial(r_1-g_1)}{\partial N}\right]^{-1}, \quad \tau_2 \equiv \left[\frac{\partial(g_2-r_2)}{\partial N}\right]^{-1}, \qquad (5)$$

and $N$ is the number of electrons in the well. In Eq. (4), the first (second) right hand side (rhs) term can be interpreted as the noise contribution of the first (second) barrier.

From Eq. (1) and (4), we can write the Fano factor $\gamma$ as

$$\gamma \equiv \frac{S}{2qI} = \left(\frac{\tau_1}{\tau_1+\tau_2}\right)^2 \frac{r_1+g_1}{r_1-g_1} + \left(\frac{\tau_2}{\tau_1+\tau_2}\right)^2 \frac{g_2+r_2}{g_2-r_2}. \qquad (6)$$

For the sake of brevity, let us define $\gamma_1$ as the first term on the rhs of Eq. (6) and $\gamma_2$ as the second, so that we can write $\gamma=\gamma_1+\gamma_2$. As we stated above, we can consider $g_1=0$ at bias voltages of interest, so that the second fraction in $\gamma_1$ is unity. As a consequence, it is straightforward to see that if we remove the Pauli blocking factors in the computation of the transition rates, all of the terms in Eq. (6) are unchanged, except for $(g_2+r_2)$ in $\gamma_2$, which increases because the individual transition rates are increased.

We should therefore expect that, when the Fano factor is dominated by $\gamma_2$, we would be able to observe the specific suppression of shot noise due to Pauli blocking, and—possibly—to clarify whether Pauli blocking factors need to be included in the individual current components.

## III. EXPERIMENT

The semiconductor heterostructure was grown by molecular-beam epitaxy on an $n$-doped GaAs(001) substrate ($n=10^{18}$ cm$^{-3}$) with the following layer structure: a 500-nm-thick Si-doped ($n=1.5\times10^{18}$ cm$^{-3}$) GaAs buffer layer, an undoped 20-nm-thick GaAs spacer layer, an undoped 11.8-nm-thick $Al_{0.35}Ga_{0.65}As$ first barrier, an undoped 5.6-nm-thick GaAs quantum well, an undoped 13.6-nm-thick $Al_{0.35}Ga_{0.65}As$ second barrier, an undoped 20-nm-thick GaAs spacer layer, and a 500-nm-thick Si-doped ($n=1.5\times10^{18}$ cm$^{-3}$) GaAs top layer. A transmission electron microscopy (TEM) image has been used for extracting layer thicknesses. However, since layer interfaces exhibited some roughness, thicknesses were finely tuned by one atomic layer by fitting the experimental data with simulations. On the other hand, simulated $I$-$V$ characteristics exhibit a large sensitivity to device and material parameters. Several devices have been fabricated on the heterostructure by the definition of top Ohmic contacts and etching mesas by standard photolithography. The collector contact was realized by metalizing the whole substrate base.

The layer sequence was chosen in order to obtain a large differential resistance, which was required as a result of the characteristics of the ultralow-noise amplifiers we had available. This, however, involves extremely low current levels at the lower end of the bias region of interest, requiring the development of a specialized procedure, with extremely high sensitivity and insulation from mechanical vibrations of different origin. The two main sources of mechanical noise are the ebullition of liquid helium, which occurs if the sample is immersed in it, and vibrations transmitted from the floor to the dewar vessel, exciting resonant modes of the structure. Such sources of spurious noise contribute mainly to the lower part of the spectrum (below 100 Hz) and are particularly disruptive for measurements performed with the highest gain. With such a configuration, the bandwidth is very limited (tens of hertz) due to the capacitances of the cables and of the capacitor used to measure the transfer function, and therefore is completely occupied by the spurious noise.

The problem with ebullition noise has been avoided by suspending the sample, mounted on a copper thermal ballast, a few millimeters above the surface of liquid helium, so that there is no direct contact. The actual temperature of the sample is monitored with a calibrated diode and kept between 5.5 and 6 K, finely adjusting the vertical position of the sample holder.

Mechanical disturbances transmitted through the floor of the shielded room in which measurements are performed have been significantly reduced, suspending the dewar on a purposely designed floating platform resting on four air-cushioned cylinders. This, along with the measurement method outlined below, has allowed reliable measurements of the shot noise associated with currents as low as 0.7 pA.

Amplification has been performed with the cross-correlation technique, i.e., connecting two identical amplifiers to the sample and evaluating the cross spectrum of their output signals,[15] in order to reduce the uncorrelated noise contributions from the amplifiers. This is necessary because, although the feedback resistors are cooled down at about 6 K, their residual thermal noise cannot be neglected in some cases in comparison with the measured shot-noise levels. Since, particularly at the lowest bias voltages of interest, we have to deal with very high device impedances (up to the gigaohm range), the main contribution from the amplifiers is associated with their equivalent input noise current sources $I_n$; therefore, we have chosen the "series" configuration reported in Fig. 2. With this choice, due to the very large ratio of the RTD impedance to the input impedance of the transresistive amplifiers, $I_n$ has a negligible effect on the other amplifier. It is therefore possible to suppress the contribution of such sources, if a large enough number of averages of the

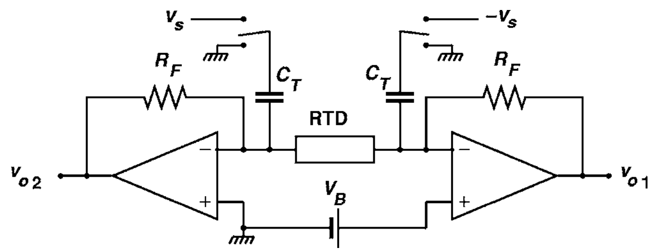


FIG. 2. Schematic diagram of the correlation amplifier used for the measurements.

cross spectrum are performed.[15,16] The switches indicated in the circuit are used to modify the configuration to precisely measure the transimpedance between the shot-noise current source of the RTD and the outputs.[16,17]

Another important step is the calibration for the measurement of the DC bias, which is particularly critical at currents below a few tens of picoamperes. Current readout is performed on the basis of the DC transimpedance of the amplifier that has the noninverting input grounded: such a transimpedance is dependent on the exact temperature of the feedback resistor and is evaluated before and after each shot-noise measurement according to the procedure outlined in Ref. 16.

The results are presented in Fig. 3, where the Fano factor is reported as a function of the bias voltage: a structure characterized by two minima for bias voltages smaller than that (242 mV) corresponding to the current peak is clearly visible. Moving backward, we observe a minimum of about 0.5 at the peak bias, then the Fano factor increases up to about 0.7 at 210 mV to decrease down to a minimum of 0.57 around 170 mV and to reach a maximum of about 0.7 again at 130 mV. Experimental results for two samples obtained on the same wafer are reported, and a good reproducibility of the data can be observed. In the same figure, we report also the DC current-voltage characteristic: the current spans 5 orders of magnitude in the voltage range considered (from 0.7 pA to 60 nA).

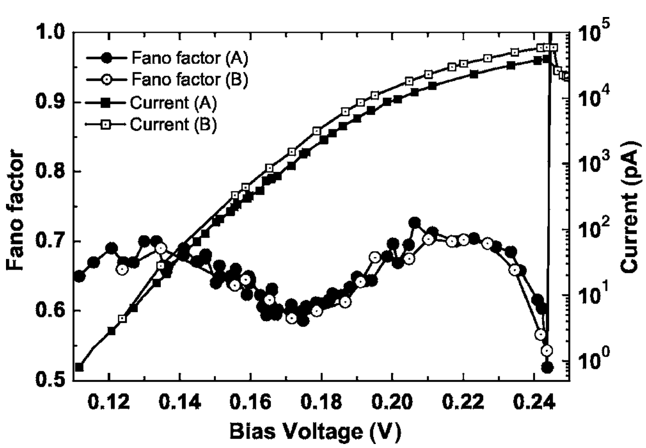


FIG. 3. Experiment: Fano factor (circles) and current (squares) as a function of the bias voltage measured at a temperature of 6 K for two different samples, A (white symbols) and B (black symbols). The current peak is at a bias of 242 mV, beyond which the Fano factor increases well above unity.

A qualitative explanation of the behavior of the Fano factor can be given by considering Eq. (6) and will be then confirmed by means of numerical simulations. At low applied voltage, we have $\tau_2 > \tau_1$, even if barrier 1 is slightly thicker than barrier 2, because on the average electrons tunneling through barrier 2 experience a higher potential barrier, and tunneling through barrier 2 is suppressed due to the mismatch of the density of initial and final states (the resonant level in the well is above the Fermi energy of the emitter). In this condition, the term $\gamma_2$ is predominant. When the bias voltage is increased, the effective barrier height decreases, and both $\tau_1$ and $\tau_2$ decrease. However, $\tau_2$ decreases faster than $\tau_1$, due to the fact that the resonant level in the well approches the emitter Fermi level, thereby increasing transition rates through barrier 2. At some point, we therefore have $\tau_1 = \tau_2$, that, in the ideal case in which $r_2 = 0$, would lead to $\gamma_1 = \gamma_2 = 0.25$ and to the well-known theoretical minimum $\gamma = 0.5$. Since in practice $r_2$ is not negligible with respect to $g_2$, we only observe a minimum of $\gamma$ that approaches 0.5 (in our case, the experimental minimum is $\gamma = 0.57$ at $V = 0.17$ V).

When the bias voltage is increased above that value, we have $\tau_1 > \tau_2$ and therefore $\gamma_1$ becomes predominant, leading to a new increase in $\gamma$. Finally, when the bias voltage moves close to the peak voltage, the resonant level in the well starts to move below the emitter conduction band, and reducing the number of states in the well available for a transition through barrier 2, $\tau_2$ increases again and diverges to infinity at the peak voltage [see Eq. (5)]. Slightly before the peak voltage, we will have again $\tau_1 = \tau_2$ and $\gamma \approx 0.5$ (now $r_2$ is vanishingly small).

On the basis of the above considerations, we expect Pauli blocking to play a role in the suppression of shot noise for bias voltages smaller than that of the first peak through $g_2$ and $\tau_2$.

## IV. INTERPRETATION

We can now consider the numerical simulations of the diode under investigation: all generation and recombination rates are computed, as described in detail in Refs. 4 and 14, on the basis of a one-dimensional (1D) Poisson-Schrödinger solver (NANOTCAD 1D) based on the effective-mass approximation, which allows us to consider quantum confinement both in the emitter and in the well and to compute each transition rate separately. The current-voltage characteristics are plotted in Fig. 4. As can be seen, the peak voltage is well reproduced in the simulation results; the magnitude of the current, on the other hand, is extremely sensitive to small parameter variations, as testified also by the significant difference between samples A and B, which are nominally identical and adjacent on the same die.

The theoretical values for $\gamma_1$, $\gamma_2$, and $\gamma$ are plotted in Fig. 5 as a function of the bias voltage. The subscript "Pauli" ("No Pauli") indicates that Pauli blocking has (has not) been included in the evaluation of the transition rates. In the considered bias voltage range, $\gamma_1$ is not affected by Pauli blocking.

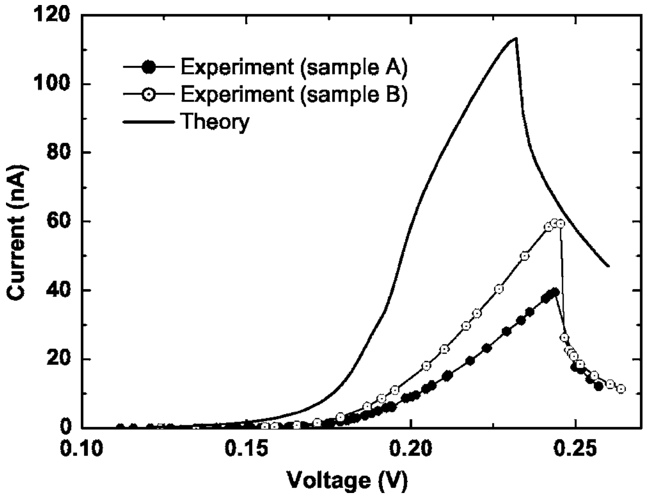


FIG. 4. Experimental current-voltage characteristics measured at 6 K of samples A and B, and characteristics obtained from numerical simulation.

The two minima of $\gamma$ are clearly noticeable, and the effect of Pauli blocking can be seen for bias voltages smaller than the first minimum of $\gamma$, leading to an additional suppression of shot noise by an amount close to 0.1. Let us also note that the voltage corresponding to the current peak is 0.232 V from simulations and 0.242 V from experiments: we believe that the difference is mainly due to poor knowledge of the doping profiles and to the fact that layer interfaces are not completely flat. The main features of the experiment can, however, be clearly interpreted and reproduced.

Finally, in Fig. 6, we plot the experimental and the theoretical Fano factors as a function of the normalized bias voltage, i.e., the bias voltage divided by the voltage corresponding to the current peak. It is apparent that the theoretical suppression factor reproduces more closely the experiments when Pauli blocking is taken into account in the evaluation of the transition rates.

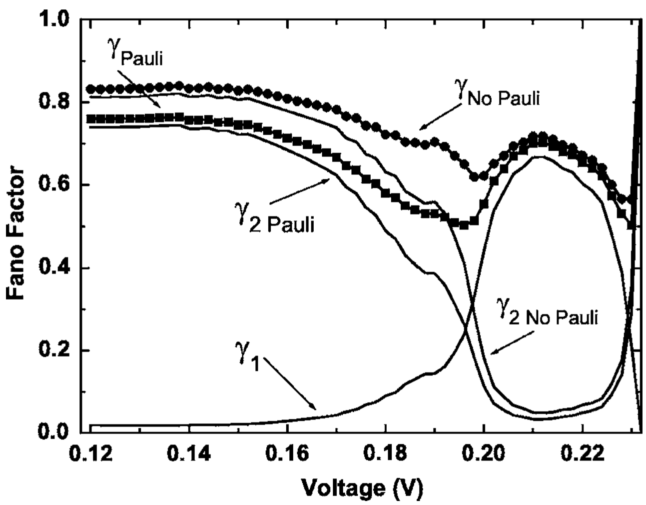


FIG. 5. Theory: Fano factor as a function of the bias voltage at 6 K when Pauli blocking is included ($\gamma_{\mathrm{Pauli}}$) and when it is not included ($\gamma_{\mathrm{No\ Pauli}}$). The Fano factor is the sum of the contributions of the two barriers: $\gamma = \gamma_1 + \gamma_2$. We plot also $\gamma_{2\ \mathrm{No\ Pauli}}$, $\gamma_{2\ \mathrm{Pauli}}$, and $\gamma_1$ ($\gamma_1$ is not affected by Pauli blocking in this voltage range). At 0.232 V, the Fano factor abruptly increases over unity.

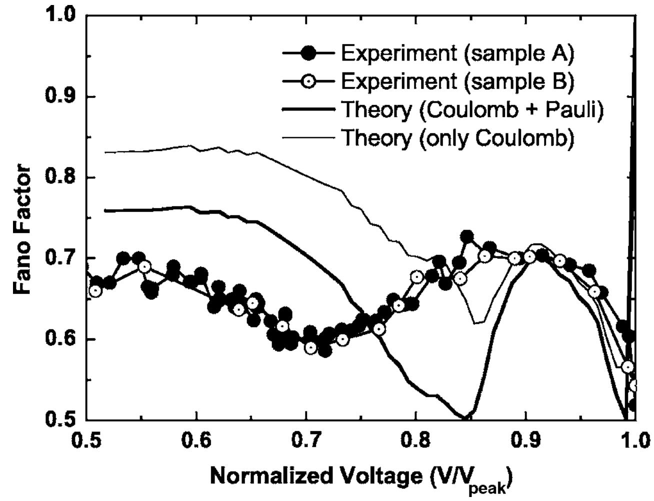


FIG. 6. The experimental Fano factors measured at 6 K for samples A and B are plotted as a function of the normalized bias voltage and compared with the theoretical Fano factor computed by including Pauli blocking ("Coulomb+Pauli") and by not including Pauli blocking ("only Coulomb"). The normalized voltage is the applied voltage divided by the voltage corresponding to the current peak.

## V. CONCLUSION

We have measured the shot-noise power spectral density of a resonant tunneling diode in a bias current range of 5 orders of magnitude, down to the subpicoampere regime, and we have revealed a double minimum structure of the Fano factor that some of us had theoretically predicted seven years ago. We have explained such a structure on the basis of an intuitive picture and of detailed numerical simulations, and have shown that the Fano factor is clearly affected by the action of the Pauli blocking principle for bias voltages smaller than that corresponding to the first minimum. Indeed, our experimental results also seem to support the view that the Pauli blocking factor has to be considered in the evaluation of the current components in a mesoscopic device, an issue that had been raised in Refs. 11 and 12. In addition, the experiment proposed in Ref. 12 to probe Pauli blocking factors would certainly provide an important further element to clarify the issue, because in that case it could be possible to tune the carrier lifetime in the central region, and therefore to verify whether the relevance of the Pauli blocking factor depends also on wave-function coherence.

## ACKNOWLEDGMENT

This work has been supported by the Italian Ministry for Education, University and Research, through the FIRB project "Nanotechnologies and Nanodevices for the Information Society" at CNR-IEIIT.

[1] W. Schottky, Ann. Phys. **57**, 541 (1918).
[2] Ya. M. Blanter and M. Büttiker, Phys. Rep. **336**, 1 (2000).
[3] Y. P. Li, A. Zaslavsky, D. C. Tsui, M. Santos, and M. Shayegan, Phys. Rev. B **41**, 8388 (1990).
[4] G. Iannaccone, G. Lombardi, M. Macucci, B. Pellegrini, Phys. Rev. Lett. **80**, 1054 (1998).
[5] Ya. M. Blanter and M. Büttiker, Phys. Rev. B **59**, 10217 (1999).
[6] W. Song, E. E. Mendez, V. Kuznetsov, and B. Nielsen, Appl. Phys. Lett. **82**, 1568 (2003).
[7] L. Y. Chen and C. S. Ting, Phys. Rev. B **43**, 4534 (1991).
[8] G. Iannaccone, M. Macucci, and B. Pellegrini, UNSOLVED PROBLEMS OF NOISE AND FLUCTUATIONS: UPoN'99: Second International Conference, AIP Conf. Proc. No. 511, (AIP, New York, 2000), pp. 59–69.
[9] V. Ya. Aleshkin, L. Reggiani, Phys. Rev. B **64**, 245333 (2001).
[10] G. Iannaccone, M. Macucci, G. Basso, and B. Pellegrini, in *Proceedings of the International Conference Noise and Fluctuations ICNF 2003*, edited by J. Sikula (CNRL s.r.o., Prague, Czech Republic, 2003), p. 283.
[11] S. Datta and M. P. Anantram, Phys. Rev. B **45**, 13761 (1992).
[12] M. Wagner, Phys. Rev. Lett. **85**, 174 (2000).
[13] R. Landauer, Nature (London) **392**, 658 (1998).
[14] G. Iannaccone, M. Macucci, and B. Pellegrini, Phys. Rev. B **56**, 12104 (1997).
[15] M. Sampietro, L. Fasoli, and G. Ferrari, Rev. Sci. Instrum. **70**, 2520 (1999).
[16] B. Pellegrini, G. Basso, and M. Macucci, *Proceedings of the International Conference Noise and Fluctuations ICNF 2003*, edited by J. Sikula (CNRL s.r.o., Prague, Czech Republic, 2003), p. 693.
[17] M. Macucci and B. Pellegrini, IEEE Trans. Instrum. Meas. **40**, 7 (1991).